

Are Negative Samples Necessary in Entity Alignment? An Approach with High Performance, Scalability and Robustness

Xin Mao^{1*}, Wenting Wang², Yuanbin Wu¹, Man Lan^{1*}
 xmao@stu.ecnu.edu.cn, {wenting.wang}@lazada.com, {ybwu,mlan}@cs.ecnu.edu.cn
¹East China Normal University & ²Alibaba Group, China & Singapore

ABSTRACT

Entity alignment (EA) aims to find the equivalent entities in different KGs, which is a crucial step in integrating multiple KGs. However, most existing EA methods have poor scalability and are unable to cope with large-scale datasets. We summarize three issues leading to such high time-space complexity in existing EA methods: (1) Inefficient graph encoders, (2) Dilemma of negative sampling, and (3) "Catastrophic forgetting" in semi-supervised learning. To address these challenges, we propose a novel EA method with three new components to enable high Performance, high Scalability, and high Robustness (PSR): (1) Simplified graph encoder with relational graph sampling, (2) Symmetric negative-free alignment loss, and (3) Incremental semi-supervised learning. Furthermore, we conduct detailed experiments on several public datasets to examine the effectiveness and efficiency of our proposed method. The experimental results show that PSR not only surpasses the previous SOTA in performance but also has impressive scalability and robustness.

CCS CONCEPTS

• **Computing methodologies** → **Neural networks; Natural language processing; Knowledge representation and reasoning.**

KEYWORDS

Knowledge Graph, Graph Neural Networks, Entity Alignment

ACM Reference Format:

Xin Mao^{1*}, Wenting Wang², Yuanbin Wu¹, Man Lan^{1*}. 2018. Are Negative Samples Necessary in Entity Alignment? An Approach with High Performance, Scalability and Robustness. In *Woodstock '18: ACM Symposium on Neural Gaze Detection*, June 03–05, 2018, Woodstock, NY. ACM, New York, NY, USA, 11 pages. <https://doi.org/10.1145/1122445.1122456>

1 INTRODUCTION

Knowledge graphs (KGs) have facilitated many downstream applications, such as recommendation [4, 37] and question-answering systems [28, 44]. In KGs, the real-world facts are presented as triples (h, r, t) . Over recent years, a large number of KGs have sprung up and been successfully applied to multiple fields. These KGs are constructed from different data sources and languages by different organizations, so they usually hold unique information individually

Permission to make digital or hard copies of all or part of this work for personal or classroom use is granted without fee provided that copies are not made or distributed for profit or commercial advantage and that copies bear this notice and the full citation on the first page. Copyrights for components of this work owned by others than ACM must be honored. Abstracting with credit is permitted. To copy otherwise, or republish, to post on servers or to redistribute to lists, requires prior specific permission and/or a fee. Request permissions from [permissions@acm.org](https://permissions.acm.org).

Woodstock '18, June 03–05, 2018, Woodstock, NY
 © 2018 Association for Computing Machinery.
 ACM ISBN 978-1-4503-XXXX-X/18/06...\$15.00
<https://doi.org/10.1145/1122445.1122456>

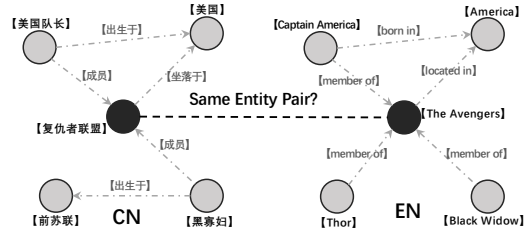


Figure 1: An example of cross-lingual entity alignment.

but also share an overlapping part in between. Clearly, integrating them offers a broader view, which has been proven effective in some applications such as search engines and cross-border E-commerce. For example, integrating cross-lingual KGs provides an opportunity to benefit the minority language users who usually suffer from lacking language resources. Therefore, how to fuse knowledge from various KGs has attracted increasing attention.

As shown in Figure 1, entity alignment (EA) aims to find the equivalent entities in different KGs, which is a crucial step in integrating multiple KGs. With the incorporation of advanced techniques, the performances of EA methods are significantly improved over the past years. But on the other hand, the computation costs are also rapidly growing in terms of time and space complexity. Zhao et al. [45] conduct an efficiency comparison of existing EA methods on a public dataset (DWY100K) that contains 100,000 entity pairs and near one million triples. In terms of time complexity, most advanced EA methods [3, 15, 33, 42] need to take more than 6 hours for training and prediction, and several [41] even take days. In terms of space complexity, several methods [3, 22, 46] require large memory consumption, so they are unable to run on a GPU with 12 GB memory, even if setting with a minimum batch size. Such poor time-space scalability hinders the application of existing EA methods to real-world datasets, which usually contain millions of entities and billions of triples (e.g., the full DBpedia contains 6.6+ million entities, 23+ billion triples). We observe three issues below in existing EA methods and believe these are the causes of the above mentioned high time-space complexity bottleneck:

(1) **Inefficient graph encoders:** Graph Neural Networks (GNNs) have become increasingly popular in addressing graph-based applications, including EA. The core of GNNs is that each node receives information from its adjacent nodes to update the structure-based embedding. But with the expansion of receptive region (i.e., graph depth), the number of support nodes (and thus the time-space complexity) increases exponentially, a.k.a. "Neighbor Explosion." Many graph sampling methods have been proposed to tackle this problem [5, 10, 43]. However, these sampling methods only work on homogeneous graphs and ignore the types of edges, which usually capture important meta information.

In addition, many complicated techniques are adopted to improve performance, e.g., Graph Matching Networks [23] and Joint Learning [3]. The overall architectures of EA methods become more and more complex, while the time complexity is also dramatically increased. For example, the running time of complex encoders (e.g., MuGNN [3]) is ten times more than that of the vanilla GCN [38].

(2) **Dilemma of negative sampling:** As a representation learning task, EA relies on margin-based pairwise loss functions (e.g., Triplet loss [30], Contrastive loss [16], or TransE [1]). In early studies [32, 38], negative samples are usually generated by uniform sampling and thus highly redundant. During training stage, the model could be hampered by such low-quality negative samples, resulting in slow convergence and performance degradation. Therefore, many previous studies focus on generating high-quality samples (i.e., hard samples), such as Top- k loss [12] and Focal loss [24]. In the EA task, BootEA [33] presents *Truncated Uniform Negative Sampling Loss* to choose k -nearest neighbors as the hard negative samples. Many subsequent studies [3, 46] adopt this simple but effective strategy. However, ranking all entities to find k -nearest neighbors in every epoch is extremely resource-consuming. For instance, the sampling stage of BootEA takes up more than 25% of the total time cost. Moreover, a large number of negative samples implicitly link to a massive GPU memory requirement. With the data scale further expanding from experimental datasets to real KGs, how to balance between performance and time-space consumption would become a dilemma.

(3) **"Catastrophic forgetting" in semi-supervised learning:** "Catastrophic forgetting" refers to the phenomenon that the networks forget the previously learned samples when learning new samples. In practice, it is expensive to label aligned entity pairs manually. Therefore, existing EA studies [33, 38, 39] usually reserve 30% of the dataset or even less as the training data to simulate this situation. Several EA methods [26, 33] introduce iterative strategies to produce semi-supervised data, which significantly boosts up the performance. However, due to the "catastrophic forgetting", existing semi-supervised EA methods have to mix up all the previously learned data with newly generated semi-supervised data and then re-train them altogether in the next iteration. Thus, the running time of such iterative semi-supervised methods is usually several times more than that of a non-iterative method. With the expansion of the data scale, time consumption would continue to increase.

The above three challenges lead to the poor scalability of existing EA methods, rendering them infeasible for large-scale KGs. In this paper, to address these challenges, we design the following three proposals: (1) Remove inefficient components from existing EA methods to greatly simplify the graph encoder architecture and adopt a new graph sampling strategy based on relational attention mechanism. (2) Inspired by recent contrastive image representation learning (CIRL) studies on the necessity of negative samples (BYOL [14] and SimSiam [9]), we prove from another angle that the essence of GNNs-based EA methods is to solve a permutation matrix approximately and the negative samples are unnecessary in EA. Based on this important finding, we design a symmetric negative-free alignment loss to improve the space and time efficiency significantly. (3) To address the "catastrophic forgetting" phenomenon and further speed up the training speed, we demonstrate a new incremental semi-supervised learning strategy. When

learning newly generated semi-supervised samples, the model only needs to review a tiny amount of the previous samples but still learns effectively. By incorporating the above three new components, we present a novel EA method with high Performance, high Scalability, and high Robustness (PSR).

To fully validate our proposed method, we conduct comprehensive experiments on several public datasets. In terms of performance, the proposed method beats all state-of-the-art competitors across all datasets. In ablation experiments, the performance of PSR only fluctuates by 3%, showing strong robustness on various hyper-parameter settings. Most importantly, PSR demonstrates impressive scalability. Its space complexity is only proportional to the batch size and graph density, while totally independent of the graph scale. Meanwhile, its time complexity only increases linearly in accordance with the graph scale. Under the same hardware environment condition, the speed of PSR is several times or even tens of times faster than other EA methods. With a small batch size (128), our proposed method could run with only 3 GB memory, while the performance is still comparable to SOTA (i.e., only degrading by less than 3%). Our main contributions are summarized as follows:

- To our best knowledge, this is the first work to prove that the essence of GNNs-based EA methods is to solve a permutation matrix approximately and explain why negative samples are unnecessary from a new angle of view.
- We propose a novel EA method with high Performance, high Scalability, and high Robustness (PSR), incorporating three components: (1) Simplified graph encoder with relational graph sampling. (2) Symmetric negative-free alignment loss. (3) Incremental semi-supervised learning.
- We design detailed experiments to examine the proposed method from multiple perspectives. The experimental results show that PSR not only surpasses the previous SOTA in performance but also has impressive scalability and robustness.

2 TASK DEFINITION

KGs store the real-world knowledge in the form of triples (h, r, t) . A KG could be defined as $G = (E, R, T)$, where E and R represent the entity set and relation set respectively, $T \subset E \times R \times E$ denotes the triple set. Defining G_1 and G_2 to be two KGs, S is the set of pre-aligned entity pairs between G_1 and G_2 . The task of EA aims to find new aligned pairs set S' based on the pre-aligned seeds S .

3 RELATED WORK

3.1 Entity Alignment

Most of existing EA methods can be summarized into two steps: (1) Using KG embedding methods (e.g., TransE [1], GCN [20], and GAT [36]) to generate low-dimensional embeddings for entities and relations in each KG. (2) Mapping these embeddings into a unified vector space through pre-aligned entities and pairing each entity by distance metrics (e.g., *Cosine* and *Manhattan*). In addition, several methods apply iterative strategies [26, 33] to generate semi-supervised data or introduce extra literal information [13, 40, 41] (e.g., entity name) to enhance the model. In Table 1, EA methods are categorized based on what design is chosen for encoder and mapper and whether introducing the enhancement module.

Method	Encoder	Mapper	Enhancement
GCN-Align [38]	GNN	Margin	None
MuGNN [3]	Hybrid	Margin	None
RSNs [32]	Trans	Corpus fusion	None
HyperKA [31]	GNN	Margin	None
BootEA [33]	Trans	Corpus fusion	Semi
NAEA [46]	Hybrid	Corpus fusion	Semi
TransEdge[34]	Trans	Corpus fusion	Semi
MRAEA [26]	GNN	Margin	Semi
GM-Align [41]	GNN	Margin	Entity Name
RDGCN [39]	GNN	Margin	Entity Name
HMAN [42]	GNN	Margin	Attribute
DGMC [13]	GNN	Margin	Entity Name

Table 1: Categorization of some popular EA methods.

Graph Encoders. *Trans* represents TransE [1] and its derivative algorithms. These methods interpret relations as a translation from head entities to tail entities and assume that the embeddings of entities and relations follow the assumption $h+r \approx t$. Due to its easy implementation and high efficiency, the *Trans* family is widely used in early EA methods. In recent studies, GNNs gradually become the mainstream encoder because of their powerful graph modeling capability. Furthermore, several EA methods adopt the *Hybrid* strategy, i.e., using GNNs to model KGs and optimizing the *Trans* loss at the same time. However, *Hybrid* methods usually require careful tuning on excessive hyper-parameters (e.g., NAEA has more than ten hyper-parameters), which leads to poor scalability and weak robustness.

Mappers. *Margin* indicates a series of margin-based pairwise losses, such as Triplet loss [30] and Contrastive loss [16], which are often used in Siamese networks [2]. Almost all GNNs-based EA methods adopt Siamese architectures with margin-based losses, which is quite similar to CIRL methods. *Corpus fusion* uses the pre-aligned set to swap the entities in existing triples and generates new triples to anchor the entities into a unified vector space. For example, there are two triples $(e_1, r_1, e_2) \in KG_1$ and $(e_3, r_2, e_4) \in KG_2$. If $(e_1, e_3) \in S$ holds, *Corpus fusion* will add two extra triples (e_3, r_1, e_2) and (e_1, r_2, e_4) . *Trans* methods usually apply such kind of mapper.

Enhancement. Due to the lack of labeled data, several methods [26, 33, 46] adopt iterative strategies to construct semi-supervised data. Despite significant performance improvements, the time consumption of these methods increases several times more. Besides, some methods [39, 41, 42] include literal information (e.g., entity name) to provide a multi-aspect EA view. However, literal information is not always available in real applications. For example, there will be privacy risks when using user-generated content.

3.2 Contrastive Image Representation Learning

The core idea of contrastive learning is to model samples through Siamese networks [2], attract positive sample pairs, and repulse negative sample pairs. This methodology has been widely utilized in self-supervised image representation learning. Recent CIRL[8, 9, 14] methods define the inputs as two augmentations of one image and

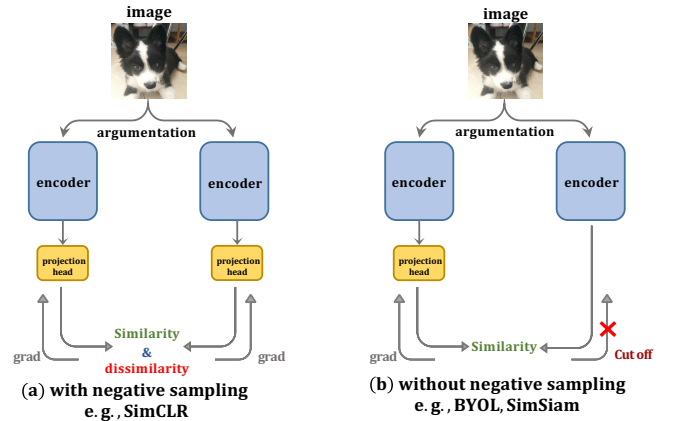


Figure 2: Examples of contrastive learning methods.¹

maximize the similarity subject to different conditions (as shown in Figure 2). The projection head is to reduce the loss of information induced by the contrastive losses. In practice, contrastive learning methods could benefit from a large number of negative samples, which require massive memory. For example, SimCLR [8] regards all the other samples in the current batch as the negative samples, and the batch size is set to 8, 192 for best performance. Obviously, most researchers can not afford the cost of such large-scale hardware resources. MoCo [18] presents the "momentum encoder" to alleviate this problem, but negative sampling remains to be the bottleneck. More recently, BYOL [14] and SimSiam [9] successfully prove that negative sampling is unnecessary for image contrastive learning by blocking half of the back-propagation stream (Figure 2b).

GNNs-based EA methods also rely on Siamese architecture with contrastive losses, so we believe that EA may also benefit from removing negative sampling, especially considering the space and time spent to find hard negative samples.

4 RETHINKING OF ENTITY ALIGNMENT

Recently, GNNs-based methods have become the mainstream of EA approaches. Taking the very first and also the simplest GNNs-based EA method, GCN-align [38] as an example, it embeds each KG into a low-dimensional space via the following equation:

$$\mathbf{H}^{(l+1)} = \sigma(\tilde{\mathbf{A}}\mathbf{H}^{(l)}\mathbf{W}^{(l)}) \quad (1)$$

where $\tilde{\mathbf{A}} \in \mathbb{R}^{|E| \times |E|}$ is the symmetric normalized Laplacian matrix, σ is an activation function, $\mathbf{H}^{(l)} \in \mathbb{R}^{|E| \times d}$ is the entity embedding matrix from the last layer, and $\mathbf{W}^{(l)}$ is a transformation matrix. Note that $\mathbf{H}^{(0)}$ is randomly initialized. Then, these entity embeddings from two KGs are mapped into a unified space via Triplet loss:

$$L = \sum_{(e_i, e_j) \in S} \left[\gamma + \|\mathbf{h}_{e_i} - \mathbf{h}_{e_j}\| - \|\mathbf{h}_{e'_i} - \mathbf{h}_{e'_j}\| \right]_+ \quad (2)$$

where (e_i, e_j) is a pre-aligned pair, (e'_i, e'_j) represents a negative pair generated by replacing one of (e_i, e_j) , γ is the margin hyper-parameter, and $[x]_+$ indicates $\max(x, 0)$. Of course, the actual implementation is more complicated, but the core idea can be summarized as the above. Naturally, there is a question raised: *What is implicitly optimized in GNNs-based EA methods?*

¹His name is BianBian. What a lovely puppy, isn't it?

4.1 Another Perspective of EA

Our Hypothesis: GNNs-based EA methods are implementations to solve a permutation matrix approximately.

Unlike the previous studies that regard EA as a representation learning task, we view EA from the perspective of permutation matrix solving. Assuming there is an ideal graph G containing all nodes and edges (i.e., the ground-truth graph), G_1 is just one particular graph instance constructed from G by using information extraction algorithm or manual labor. We use $\tilde{A} \in \mathbb{R}^{|E| \times |E|}$ and $\tilde{A}_1 \in \mathbb{R}^{|E| \times |E|}$ to denote the symmetric normalized Laplacian matrix of G and G_1 , respectively. Then, the construction process of G_1 from G could be described into two steps: reorder the entities in G and introduce certain noise. Formally, this construction process is formulated as below:

$$P\tilde{A}P^{-1} + N = \tilde{A}_1 \quad (3)$$

where $P \in \mathbb{R}^{|E| \times |E|}$ is a permutation matrix representing the equivalent relation of entities between G and G_1 . Note that there is exactly one entry of 1 in each row and each column in P while 0s elsewhere. Thus, P is also an orthogonal matrix, which complies with the fundamental assumption in EA that one entity has and only has one aligned entity. When $P_{ij} = 1$, it represents that $e_i \in G$ and $e_j \in G_1$ are an aligned pair. $N \in \mathbb{R}^{|E| \times |E|}$ is a noise matrix denoting the subtle noise added during the construction process of G_1 . Thus, in essence, different graph instances could be regarded as the results of the same ideal graph by changing with different orders and introducing different noises (as illustrated in Figure 3). Therefore, for two graph instances G_1 and G_2 constructed from the same ideal graph G , we have the following equation:

$$P_1^{-1}(\tilde{A}_1 - N_1)P_1 = \tilde{A} = P_2^{-1}(\tilde{A}_2 - N_2)P_2 \quad (4)$$

Let \bar{P} be the permutation matrix equaling to $P_1P_2^{-1}$. The above equation is transformed into:

$$(\tilde{A}_1 - N_1)\bar{P} = \bar{P}(\tilde{A}_2 - N_2) \quad (5)$$

Meanwhile, according to the definition of the permutation matrix, the pre-aligned entity set S is equivalent to a set of constraints:

$$[(\tilde{A}_1 - N_1)\bar{P}]_i = [\bar{P}(\tilde{A}_2 - N_2)]_j, \forall (e_i, e_j) \in S \quad (6)$$

where $[X]_i$ represents the i -th row of matrix X . Obviously, the aim of EA now turns to solve the permutation matrix \bar{P} under these constraints (i.e., given pre-aligned entity pairs S).

4.2 Approximate Matrix Solving

Both the permutation matrix \bar{P} and the two noise matrices (i.e., N_1 and N_2) are unknown high-dimensional matrices, which is hard to solve directly. Without loss of generality, the EA task follows the two premises as below:

Premise 1: Since the introduced noise is subtle, the structures of G_1 and G_2 are still isomorphic to G . Thus, the noise matrices N_1 and N_2 in Equation (6) could be dropped, approximately.

Premise 2: Approximately, the matrix \bar{P} could be further decomposed into the product of two low-rank dense matrices $M_1 \in \mathbb{R}^{|E| \times d}$ and $M_2 \in \mathbb{R}^{d \times |E|}$ (i.e., $\bar{P} \approx M_1M_2$).

Let $M_2^{rinv} \in \mathbb{R}^{|E| \times d}$ be the right inverse matrix of M_2 (i.e., $M_2M_2^{rinv} = I_d$), Equation (6) could be transformed into:

$$[\tilde{A}_1M_1]_i = [\tilde{A}_2M_2^{rinv}]_j, \forall (e_i, e_j) \in S \quad (7)$$

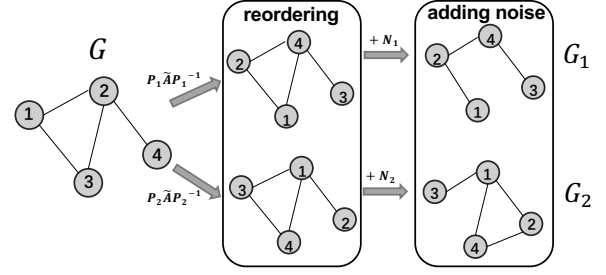


Figure 3: Construction process of G_1 and G_2 from G .

here M_1 and M_2^{rinv} must be full column rank. Obviously, when we modify the above equation by introducing an activation function σ and adding further decompositions as $M_1 = H_1W_1$ and $M_2^{rinv} = H_2W_2$, Equation (7) still holds:

$$[\sigma(\tilde{A}_1H_1W_1)]_i = [\sigma(\tilde{A}_2H_2W_2)]_j, \forall (e_i, e_j) \in S \quad (8)$$

Compared to Equation (1), we find that either side of Equation (8) is in the same form as the right-hand side of Equation (1), which suggests that the approximate matrix solving is equivalent to the Siamese networks with GCN encoders. In general, Equation (8) could be solved by the least-squares method:

$$\arg \min_{H_{1,2}, W_{1,2}} \sum_{(e_i, e_j) \in S} \left\| \sigma([\tilde{A}_1H_1W_1]_i) - \sigma([\tilde{A}_2H_2W_2]_j) \right\|_2^2 \quad (9)$$

Simply optimizing Equation (9) by gradient descent inclines to a trivial solution [9] (i.e., all outputs collapse to a constant). Therefore, it is essential to ensure that H_1W_1 and H_2W_2 are both full column rank to prevent the model from collapsing.

Generally, the involving of negative samples is equivalent to introducing a penalty term to trivial solutions, which can preclude constant outputs from the solution space. Blocking half of the back-propagation stream (i.e., Figure 2b) also avoids constant outputs. Putting this trick into our approximate solving framework, it is analogous to approximately solving \bar{P} by only updating H_1W_1 with a fixed H_2W_2 . Intuitively, in high dimensions, any randomly drawn vectors are always nearly orthogonal. Thus, H_1W_1 and H_2W_2 are invariably full column rank. In a nutshell, blocking back-propagation would guarantee that the EA models do not collapse.

4.3 Further Analysis of GNNs-based EA

In our opinion, GNNs-based EA has a close correlation with CIRL. Once we view the ideal KG as the input image, the graph instance construction process is equivalent to the random image argumentation trick. However, there are still several fundamental differences between these two tasks. For example, there is only one ideal graph in EA, but thousands of images in CIRL. These differences might be the reason that several key techniques (e.g., momentum encoder) are proved to be effective in CIRL but not working in EA.

Note that although the above inferences depend on the premise that \tilde{A} is invariant, it is easily extended into attention-based GNNs [26, 36, 39] with variant \tilde{A} . Thereby a more general inference method is derived and proved in our subsequent experiments.

5 THE PROPOSED METHOD

This section will describe our proposed method in detail, including the encoder architecture and training strategy.

5.1 Encoder Architecture

To effectively deal with large-scale KGs, we propose a minimalism relation-aware graph encoder. The proposed encoder removes all high-complexity components (e.g., *hybrid* strategy and graph matching) and even abandons the normal linear transformation matrix. The inputs of our model are two matrices: $\mathbf{H}_e^{(0)} \in \mathbb{R}^{|E| \times d}$ represents the input entity features and $\mathbf{H}_r \in \mathbb{R}^{|R| \times d}$ represents the input relation features. Both of them are initialized by the random uniform initializer. Our proposed minimalism relation-aware graph encoder consists of three major components:

Relation-specific embeddings. KG usually contains complicated relationships, such as reflexive, one-to-many, many-to-one, and many-to-many. Some KG embedding methods [25, 29] construct relation-specific entity embeddings in order to better describe these complex relations. Inspired by RREA [27], we generate reflections of entities along the relational hyperplanes to enforce relation-specificity:

$$\phi(\mathbf{h}_{e_i}, \mathbf{h}_{r_k}) = \mathbf{h}_{e_i} - 2\mathbf{h}_{r_k}^T \mathbf{h}_{e_i} \mathbf{h}_{r_k} \quad (10)$$

where \mathbf{h}_{e_i} and \mathbf{h}_{r_k} represent the embeddings of entity e_i and relation r_k , and $\|\mathbf{h}_{r_k}\|_2 = 1$. Compared with RGCN [25] and TransR [29] which set up a transformation matrix for each relation, the above operation only requires much fewer parameters and has higher computational efficiency.

Relational attention aggregator. When aggregating neighborhood information, the vanilla GCN only considers the degree of nodes and ignores the type of edges, which we believe also embeds hidden semantics. Therefore, we bring in the relational attention mechanism to distinguish the importance between edges and aggregate neighboring information anisotropically. Besides, we remove the normal linear transformation matrix and replace it with the relation-specific embeddings. The output feature of e_i from the l -th layer is described as following:

$$\mathbf{h}_{e_i}^{(l+1)} = \sigma \left(\sum_{e_j \in \mathcal{N}_{e_i}} \sum_{r_k \in R_{ij}} \alpha_{ijk}^{(l)} \phi(\mathbf{h}_{e_j}^{(l)}, \mathbf{h}_{r_k}^{(l)}) \right) \quad (11)$$

where \mathcal{N}_{e_i} is the neighboring entity set of e_i , and R_{ij} is the set of relations between e_i and e_j . In this work, we adopt ELU [11] as the activation function. $\alpha_{ijk}^{(l)}$ represents the relational attention coefficient which is obtained as below:

$$\beta_{ijk}^{(l)} = \mathbf{v}^T [\phi(\mathbf{h}_{e_i}^{(l)}, \mathbf{h}_{r_k}^{(l)}) \parallel \mathbf{h}_{r_k} \parallel \phi(\mathbf{h}_{e_j}^{(l)}, \mathbf{h}_{r_k}^{(l)})] \quad (12)$$

$$\alpha_{ijk}^{(l)} = \frac{\exp(\beta_{ijk}^{(l)})}{\sum_{e_{j'} \in \mathcal{N}_{e_i}} \sum_{r_{k'} \in R_{ij'}} \exp(\beta_{ij'k'}^{(l)})} \quad (13)$$

where $\mathbf{v} \in \mathbb{R}^{3d}$ is a trainable vector for calculating the attention coefficient. \parallel means the concatenate operation.

Multi-hop representation. To enable a global-aware representation, we concatenate the output embeddings from multiple layers,

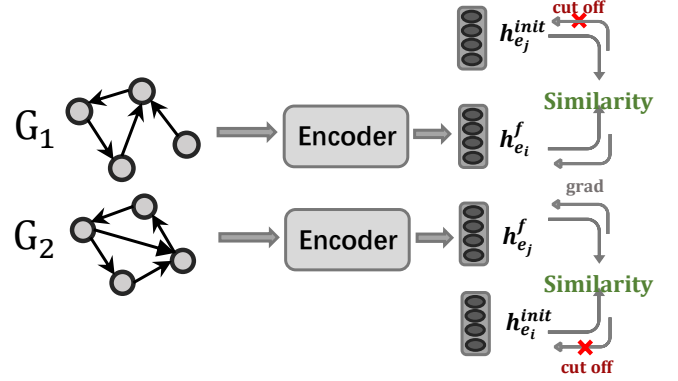


Figure 4: The illustration of symmetric negative-free loss.

capturing multi-hop neighboring information. The final output embedding of entity e_i is in the following form:

$$\mathbf{h}_{e_i}^f = [\mathbf{h}_{e_i}^{(0)} \parallel \mathbf{h}_{e_i}^{(1)} \parallel \dots \parallel \mathbf{h}_{e_i}^{(l)}] \quad (14)$$

where $\mathbf{h}_{e_i}^{(0)}$ represents the input embedding of e_i .

5.2 Training Strategy

In addition to simplifying the encoder's architecture, the proposed method also boosts the training efficiency from three aspects:

Relational attention graph sampling. Previous GNNs-based EA methods [3, 26, 38] usually train on full graph, with the consequence of demanding large memory and slow speed. Following GraphSAGE [17], we only sample a small batch of positive pairs from training data and construct a multi-hop sub-graph. But instead of the equal probability sampling, we propose an unequal probability sampling strategy since we believe not all triples have equal importance. Given the center node e_i , we sample t times from its neighboring triples with replacement and directly use the normalized attention coefficient α_{ijk} as the probability of triple (e_i, r_k, e_j) :

$$P((e_i, r_k, e_j)|e_i) = \alpha_{ijk} \quad (15)$$

With this setting, more important triples have a higher probability of being sampled. In accordance with this, for different center nodes, the expectations of attention coefficient from one sampling (also means information capacity) are different:

$$\mathbb{E}[\alpha_{e_i}] = \sum_{e_j \in \mathcal{N}_{e_i}} \sum_{r_k \in R_{ij}} P((e_i, r_k, e_j)|e_i) \alpha_{ijk} \quad (16)$$

$$= \sum_{e_j \in \mathcal{N}_{e_i}} \sum_{r_k \in R_{ij}} \alpha_{ijk}^2 \quad (17)$$

If we follow the previous studies to use a fixed t or set t inversely proportional to the degree, it will lead to redundancy or deficiency of information. In fact, we expect that for any center node e_i , the sum of attention coefficient expectations should maintain certain stability after t_{e_i} round of sampling:

$$t_{e_i} = \lceil \frac{\tau}{\mathbb{E}[\alpha_{e_i}]} \rceil \quad (18)$$

where τ is a hyper-parameter controlling the sampling ratio. $\lceil x \rceil$ denotes the ceil operation.

Datasets	DBP _{ZH}	DBP _{EN}	DBP _{JA}	DBP _{EN}	DBP _{FR}	DBP _{EN}	SRP _{EN}	SRP _{FR}	SRP _{EN}	SRP _{DE}	DWY _{DBP}	DWY _{YG}	DWY _{DBP}	DWY _{WD}
E	19,388	19,572	19,814	19,780	19,661	19,993	15,000	15,000	15,000	15,000	100,000	100,000	100,000	100,000
R	2,830	2,317	2,043	2,096	1,379	2,209	221	177	222	120	302	31	330	220
T	70,414	95,142	77,214	93,484	105,998	115,722	36,508	33,532	38,363	37,377	428,952	502,563	463,294	448,774

Table 2: Statistics of the Datasets. |E|, |R| and |T| are the size of entities, relations and triples respectively.

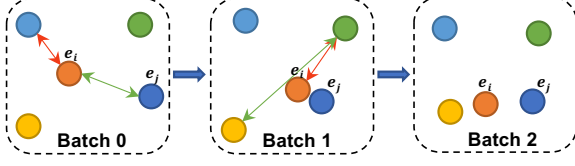


Figure 5: An example of "forgetting". Green lines represent positive pairs and red lines represent negative pairs.

Symmetric negative-free alignment loss. As mentioned in Section 4.2, one side of the Siamese networks' back-propagation should be blocked to prevent the model from collapsing in the case of no negative samples. Specifically, we first initialize the graph encoder randomly, make a forward propagation on each KG, and store the initial output embedding \mathbf{h}^f as \mathbf{h}^{init} for each entity. Next, taking \mathbf{h}^{init} as the target, the model is optimized by the following loss function (as illustrated in Figure 4):

$$L = \sum_{(e_i, e_j) \in S} -\text{sim}(\mathbf{h}_{e_i}^f, \mathbf{h}_{e_j}^{init}) - \text{sim}(\mathbf{h}_{e_j}^f, \mathbf{h}_{e_i}^{init}) \quad (19)$$

The back-propagation streams of $\mathbf{h}_{e_i}^{init}$ and $\mathbf{h}_{e_j}^{init}$ are cut off. In this paper, we use the *cosine* similarity as the metric $\text{sim}(\mathbf{x}, \mathbf{y})$.

$$\text{sim}(\mathbf{x}, \mathbf{y}) = \frac{\langle \mathbf{x}, \mathbf{y} \rangle}{\|\mathbf{x}\|_2 \|\mathbf{y}\|_2} \quad (20)$$

In fact, $\mathbf{h}_{e_i}^{init}$ and $\mathbf{h}_{e_j}^{init}$ are analogous to the target network in BYOL [14]. However, due to the fundamental differences between EA and CIRL, adopting the momentum encoder of MoCo and BYOL will cause the model to degrade. Thus, the momentum encoder is not incorporated in our model. Once the training process is completed, the final similarity score between e_i and e_j is calculated as below:

$$\text{score}(e_i, e_j) = \text{sim}(\mathbf{h}_{e_i}^f, \mathbf{h}_{e_j}^{init}) + \text{sim}(\mathbf{h}_{e_j}^f, \mathbf{h}_{e_i}^{init}) \quad (21)$$

Incremental semi-supervised learning. "Catastrophic forgetting" refers to the phenomenon that the networks forget the previously learned samples after learning new samples. Specific in the EA task, $(e_i, e_j) \in S$ is a pre-aligned pair, which has already been mapped to an adjacent space in the early training batch. However, once e_i or e_j is chosen to be negative samples, the model "forgets" their learned relative positions (as shown in Figure 5). Therefore, existing EA methods need to mix the newly generated semi-supervised data with the early training data and then retrain the model, resulting in low efficiency. With the complete absence of negative samples, the proposed method is born with the power to do incremental learning. When learning new batches, the learned entity embeddings are only indirectly influenced by their neighboring entities. Thus, the "forgetting" phenomenon is largely weakened. To further alleviate "catastrophic forgetting," we store all the embeddings of the training set after each iteration (embeddings of the previous iteration will be overwritten). In the next iteration,

Algorithm 1 Incremental Semi-supervised Learning Strategy

Input: Graphs $G_1 = (E_1, R_1, T_1), G_2 = (E_2, R_2, T_2)$, pre-aligned seed entity pairs $S^{init}, E'_1 \subseteq E_1, E'_2 \subseteq E_2$ are the candidate entity sets not existing in S^{init} .
Output: parameters θ for model
1: Initialize the model;
2: $S \leftarrow S^{init}$; /*Initialize the training set.*/
3: $Q \leftarrow \{\}$; /*Store the embeddings of all previous training pairs.*/
4: **repeat**
5: Train the model with G_1, G_2 , and S until the loss of development set increase;
6: $S^{new} \leftarrow \{\}$; /*Initialize new training set.*/
7: /*Review all the previous embeddings*/
8: **for** $(\mathbf{h}_{e_i}^{last}, \mathbf{h}_{e_j}^{last}) \in Q$ **do**
9: **if** $\text{sim}(\mathbf{h}_{e_i}^{last}, \mathbf{h}_{e_j}^{last}) - \text{sim}(\mathbf{h}_{e_i}^{now}, \mathbf{h}_{e_j}^{now}) > \epsilon$ **then**
10: $S^{new} \leftarrow S^{new} \cup \{(e_i, e_j)\}$;
11: **end if**
12: **end for**
13: /*Generate bi-directional semi-supervised aligned pairs*/
14: **for** $e \in E'_1$ **do**
15: $e' = N(e, E'_2)$ /* $N(e, E)$ is the entity nearest to e in E .*/
16: **if** $N(e', E'_1) = e$ **then**
17: $S^{new} \leftarrow \{(e, e')\} \cup S^{new}$; $E'_1 \leftarrow E'_1 - \{e\}$; $E'_2 \leftarrow E'_2 - \{e'\}$;
18: **end if**
19: **end for**
20: /*Update the embeddings set*/
21: **for** $(e_i, e_j) \in S$ **do**, $Q \leftarrow Q \cup \{(\mathbf{h}_{e_i}^{now}, \mathbf{h}_{e_j}^{now})\}$;
22: **end for**
23: $S \leftarrow S^{new}$; /*Update the training set*/
24: **until** no more aligned entities are added to S

we compare them with the currently learned embeddings. If the similarity difference of an entity pair exceeds ϵ , such pair will be added into the next iteration again (a.k.a, reviewing). According to our experiments, only very few pairs will be added multiple times.

In addition, we adopt the *Bi-directional Iterative Strategy* proposed by MRAEA [26] to construct high-quality semi-supervised aligned pairs. If and only if the entities e_i and e_j are mutually nearest neighbors to each other, then the pair (e_i, e_j) would be considered as new semi-supervised aligned entities. The detailed incremental semi-supervised procedure is described in Algorithm 1.

6 EXPERIMENTS

All the experiments are conducted on a PC with a GeForce GTX TITAN X GPU (12GB) and 128GB memory. The code is now available (<https://github.com/MaoXinn/PSR>).

6.1 Datasets

To fairly and comprehensively verify the performance, scalability, and robustness of our model, we experiment with three widely used public datasets: (1) **DBP15K** [32]: This dataset consists of three cross-lingual subsets from multi-lingual DBpedia: DBP_{EN-FR}, DBP_{EN-ZH}, and DBP_{EN-JA}. Each subset contains 15,000 pre-aligned entity pairs. As an early dataset, DBP15K is the most popular one but has two defects: small scale and dense links. (2) **SRPRS**: Guo et al. [15] propose this sparse dataset, including two cross-lingual subsets: SRPRS_{FR-EN} and SRPRS_{DE-EN}. Each subset also contains 15,000 pre-aligned pairs but with much fewer triples compared to

Method	DBP _{ZH-EN}			DBP _{JA-EN}			DBP _{FR-EN}			SRPRS _{FR-EN}			SRPRS _{DE-EN}			
	H@1	H@10	MRR	H@1	H@10	MRR	H@1	H@10	MRR	H@1	H@10	MRR	H@1	H@10	MRR	
Basic	MTransE	0.209	0.512	0.310	0.250	0.572	0.360	0.247	0.577	0.360	0.213	0.447	0.290	0.107	0.248	0.160
	GCN-Align	0.434	0.762	0.550	0.427	0.762	0.540	0.411	0.772	0.530	0.243	0.522	0.340	0.385	0.600	0.460
	MuGNN	0.494	0.844	0.611	0.501	0.857	0.621	0.495	0.870	0.621	0.131	0.342	0.208	0.245	0.431	0.310
	RSNs	0.508	0.745	0.591	0.507	0.737	0.590	0.516	0.768	0.605	0.350	0.636	0.440	0.484	0.729	0.570
	HyperKA	0.572	0.865	0.678	0.564	0.865	0.673	0.597	0.891	0.704	-	-	-	-	-	-
	PSR(basic)	0.702	0.924	0.781	0.698	0.930	0.782	0.731	0.941	0.807	0.441	0.741	0.542	0.553	0.799	0.638
	±stds	0.003	0.002	0.002	0.004	0.001	0.002	0.003	0.003	0.002	0.004	0.002	0.002	0.003	0.002	0.003
<i>p</i> -value	2e-16	8e-15	5e-17	2e-15	6e-18	3e-17	2e-16	1e-12	5e-17	8e-14	4e-17	6e-17	7e-14	2e-15	8e-14	
Semi	BootEA	0.629	0.847	0.703	0.622	0.853	0.701	0.653	0.874	0.731	0.365	0.649	0.460	0.503	0.732	0.580
	NAEA	0.650	0.867	0.720	0.641	0.872	0.718	0.673	0.894	0.752	0.177	0.416	0.260	0.307	0.535	0.390
	TransEdge	0.735	0.919	0.801	0.719	0.932	0.795	0.710	0.941	0.796	0.400	0.675	0.490	0.556	0.753	0.630
	JEANS	0.719	0.895	0.791	0.737	0.914	0.798	0.769	0.940	0.827	-	-	-	-	-	-
	MRAEA	0.757	0.930	0.827	0.758	0.934	0.826	0.781	0.948	0.849	0.460	0.768	0.559	0.594	0.818	0.666
	PSR(semi)	0.802	0.935	0.851	0.803	0.938	0.852	0.828	0.952	0.874	0.486	0.781	0.577	0.606	0.831	0.680
	±stds	0.004	0.001	0.004	0.003	0.002	0.003	0.003	0.002	0.002	0.003	0.002	0.003	0.004	0.003	0.002
<i>p</i> -value	4e-11	6e-08	1e-08	3e-12	1e-04	4e-10	2e-12	1e-04	2e-11	4e-10	6e-09	1e-08	4e-06	2e-07	3e-09	
Literal	GM-Align	0.679	0.785	-	0.739	0.872	-	0.894	0.952	-	0.574	0.646	0.602	0.681	0.748	0.710
	RDGCN	0.697	0.842	0.750	0.763	0.897	0.810	0.873	0.950	0.901	0.672	0.767	0.710	0.779	0.886	0.820
	HMAN	0.561	0.859	0.670	0.557	0.860	0.670	0.550	0.876	0.660	0.401	0.705	0.500	0.528	0.778	0.620
	HGCN	0.720	0.857	0.760	0.766	0.897	0.810	0.892	0.961	0.910	0.670	0.770	0.710	0.763	0.863	0.801
	DGMC	0.801	0.875	-	0.848	0.897	-	0.933	0.960	-	-	-	-	-	-	-
	PSR(lit)	0.883	0.982	0.928	0.908	0.987	0.939	0.958	0.997	0.975	0.808	0.933	0.853	0.881	0.970	0.914
	±stds	0.004	0.002	0.003	0.005	0.003	0.002	0.003	0.001	0.001	0.003	0.004	0.002	0.003	0.002	0.003
<i>p</i> -value	2e-13	4e-17	2e-17	2e-11	7e-15	7e-18	6e-10	1e-15	6e-18	2e-16	4e-16	3e-18	2e-15	3e-16	4e-15	

Table 3: Experimental results (Means_{±stds}) on DBP15K and SRPRS. Besides the performances, we further conduct the one-sample T-test between PSR and the best baselines. All the *p*-value < 0.01 indicates that PSR significantly outperforms all baselines.

DBP15K . (3) **DWY100K** [33]: This dataset comprises two monolingual subsets, each containing 100,000 pre-aligned entity pairs and nearly one million triples. As the largest dataset, DWY100K raises challenges to the scalability of EA models.

The statistics of these datasets are summarized in Table 2. To be consistent with previous studies [26, 33, 38, 39], we randomly split 30% of the pre-aligned entity pairs for training and development while using the remaining 70% for testing.

6.2 Baselines

To fully evaluate our proposed method, we compare it against the following three groups of advanced EA methods: (1) **Structure**: These methods only use the original structure information (i.e., triples): MTransE [7], GCN-Align [38], RSNs [15], MuGNN [3], HyperKA [31]. (2) **Semi-supervised**: These methods adopt iterative strategy to generate semi-supervised data: BootEA [33], NAEA [46], TransEdge [34], MRAEA [26], JEANS [6]. (3) **Literal**: To obtain a multi-aspect view, these methods use the literal information (e.g., entity name) of entities as the input features: GM-Align [41], RDGCN [39], HMAN [42], HGCN [40], DGMC [13].

To make a fair comparison against the above three groups of methods, PSR also has three corresponding versions: (1) PSR (basic) is the basic version without incremental learning. (2) PSR (semi) introduces incremental learning to generate semi-supervised data. (3) PSR (lit) adopts a simple strategy to incorporate the literal information. Specifically, for e_i and e_j , we first use PSR (Semi) to obtain the structural similarity ss_{ij} . Then, using the cross-lingual word embeddings (same with GM-Align [21]) to calculate the literal similarity ls_{ij} . Finally, the entities are ranked according to $ls_{ij} + ss_{ij}$.

6.3 Settings

Metrics. Following convention [7, 33, 38, 41], we use *Hits@k* and *Mean Reciprocal Rank (MRR)* as the evaluation metrics. We report the average of five independent runs as the results.

Hyper-parameters. For all datasets, the same default configuration is set: embedding dimension $d = 300$; depth of GNN $l = 2$; sampling ratio $\tau = 1$; reviewing threshold $\epsilon = 0.05$; batch size is 512; dropout rate is set to 30%. RMSprop is adopted to optimize the model with a learning rate set to 0.005.

6.4 Main Experiments

In Table 3 and Table 4, we report the performance of all methods on all three datasets. Our method consistently achieves the best performance across all datasets and metrics.

Results on DBP15K. On this dataset, PSR (basic) outperforms the previous SOTA in the Basic group by more than 13% on Hit@1 and 10% on MRR. This indicates that the architecture of PSR effectively captures the rich relational structure information existing in this dataset. Benefiting from the extra semi-supervised data, the performance of PSR (semi) is significantly improved on every metric compared to its basic version. Moreover, compared against other advanced semi-supervised EA methods, PSR (semi) still maintains a significant performance advantage of 4% on *Hits@1*. Through further incorporating of cross-lingual word embeddings, PSR (lit) could model entities from both structure and semantics perspectives. Therefore, its performance further increases and consistently surpasses the previous SOTA in the Literal group. Besides, we observe that the performances of the Literal group vary significantly across language pairs, which is entirely different from the structure-only groups. The French dataset has the most apparent gain, while the Chinese dataset has the least.

Results on SRPRS. To simulate the degree distribution in real-world data, SRPRS greatly cuts down the number of triples, which challenges EA methods' embedding capability on sparse KGs. Although the performance of PSR drops compared to DBP15K, it still outperforms all the other advanced EA methods. The semi-supervised strategy still has some benefits, but the improvement

Method	DWY _{DBP-WD}			DWY _{DBP-YG}			
	H@1	H@10	MRR	H@1	H@10	MRR	
Basic	MTransE	0.238	0.507	0.330	0.227	0.414	0.290
	GCN-Align	0.494	0.756	0.590	0.598	0.829	0.680
	MuGNN	0.604	0.894	0.701	0.739	0.937	0.810
	RSNs	0.607	0.793	0.673	0.689	0.878	0.756
	PSR(basic)	0.781	0.935	0.838	0.851	0.968	0.894
	\pm stds	0.003	0.001	0.002	0.003	0.003	0.002
p -value	1e-17	4e-16	4e-18	9e-16	9e-11	3e-16	
Semi	BootEA	0.748	0.898	0.801	0.761	0.894	0.808
	NAEA	0.767	0.918	0.817	0.779	0.913	0.821
	TransEdge	0.788	0.938	0.824	0.792	0.936	0.832
	MRAEA	0.794	0.930	0.856	0.819	0.951	0.875
	PSR(semi)	0.881	0.967	0.912	0.892	0.978	0.923
	\pm stds	0.002	0.001	0.002	0.003	0.001	0.002
p -value	2e-16	1e-15	1e-14	4e-14	2e-14	5e-14	

Table 4: Experimental results on DWY100K².

Method	DBP _{ZH-EN}		DBP _{JA-EN}		DBP _{FR-EN}	
	Hits@1	MRR	Hits@1	MRR	Hits@1	MRR
PSR(semi)	0.802	0.851	0.803	0.852	0.828	0.874
-RSE.	0.790	0.841	0.774	0.828	0.806	0.854
-RAA.	0.789	0.842	0.785	0.841	0.809	0.862
-MHR.	0.751	0.817	0.750	0.815	0.789	0.847
-RAGS.	0.789	0.843	0.788	0.844	0.816	0.868
-SNAL.	0.799	0.850	0.798	0.847	0.830	0.876

Table 5: Ablation experiments of model architecture.

is reduced to 4-5%. We believe the reason for this smaller improvement is that the sparse nature of SRPRS makes the generation of high-quality semi-supervised data very hard. Therefore, the literal information becomes critical on SRPRS and improves *Hits@1* by at least 28% if compared to PSR (semi).

Results on DWY100K. As the largest dataset, DWY100K raises challenges to the space-time complexity of EA methods. MuGNN and NAEA exceed the GPU memory limit setup in this experiment, so they have to run on the CPU, which substantially slows down the training speed. On the contrary, the high scalability enables our model easy to cope with this large dataset and surpasses the previous SOTA by at least 7% on *Hits@1* (shown in Table 4). In addition, since this dataset shares similar dense degree distribution with DBP15K, the semi-supervised strategy also works well here.

Time Efficiency. The trump card of PSR is superior efficiency and scalability. So we specifically evaluate the overall time costs of existing EA methods and report all results in Table 6. It is obvious that the efficiency of PSR far exceeds all advanced competitors. The speed of our proposed method is tens or even hundreds of times faster than that of existing complex EA methods. Even compared against the fastest baseline (i.e., GCN-Align), the speed of PSR (basic) is 5 \times faster on DWY100K, while the *Hits@1* is 25% higher. Among the PSR group itself, the semi-supervised strategy consumes 2 \times more time cost than the basic version, while PSR (lit) has no clear additional time cost than PSR (semi).

²According to Zhao et al. [45], entity names between mono-lingual KGs for this dataset are almost identical and the edit distance algorithm could achieve the ground-truth performance. Therefore, the experimental results of literal methods are not listed.

Method	DBP15K	SRPRS	DWY100K	
Basic	MTransE [7]	6,467	3,355	70,085
	GCN-Align [38]	103	87	3,212
	RSNs [15]	7,539	2,602	28,516
	MuGNN [3]	3,156	2,215	47,735
	PSR(basic) [35]	88	75	603
Semi	BootEA [33]	4,661	2,659	64,471
	NAEA [46]	19,115	11,746	171,357
	TransEdge[34]	3,629	1,210	20,839
	MRAEA [26]	3,894	1,248	23,275
	PSR(semi) [35]	186	168	1,452
Literal	GM-Align [41]	26,328	13,032	459,715
	RDGCN [39]	6,711	886	-
	HMAN [42]	5,455	4,424	31,895
	HGCN [40]	11,275	2,504	60,005
	PSR(lit) [35]	195	183	1,532

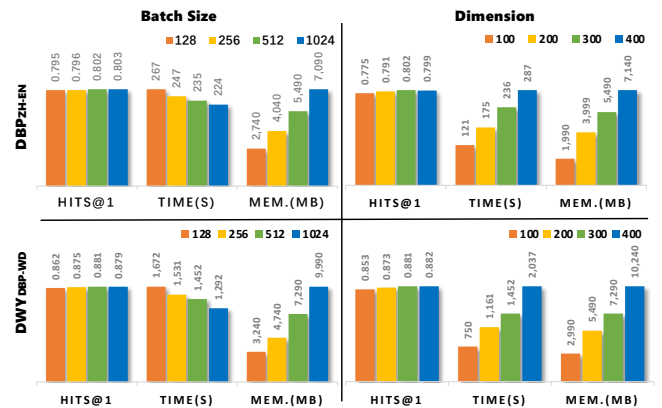
Table 6: Time costs of EA methods (seconds).³

Figure 6: Ablation experiments on batch size and dimension.

6.5 Ablation Experiment

Model Architecture. The architecture of PSR consists of the following five components: (1) *Relation-specific embeddings* (RSE); (2) *Relational attention aggregator* (RAA); (3) *Multi-hop representation* (MHR); (4) *Relational attention graph sampling* (RAGS); (5) *Symmetric negative-free alignment loss* (SNAL). We replace these components from PSR(semi) individually to demonstrate their effectiveness. Specifically, RSE is replaced by normal linear transformation matrices. RAA and RAGS become isotropic, i.e., all entities and relations have equal importance. MHR is replaced by the residual connection [19] and SNAL is replaced by the *Truncated Uniform Negative Sampling loss* [33]. The experimental results are listed in Table 5. Among all these components, MHR has the greatest impact on performance. Without MHR, the performances are degraded by at least 4% on *Hits@1*. For SNAL, the results are almost identical to the *Truncated Uniform Negative Sampling loss*, indicating that SNAL could reduce the time-space consumption without losing any accuracy. Besides, the remaining three components also show the necessity as our expectation. On average, adopting them improves performance by 1% to 3% on *Hits@1*.

³All results are obtained by directly running the source code with default settings. RDGCN requires extremely high memory space and we are unable to obtain its result on DWY100K.

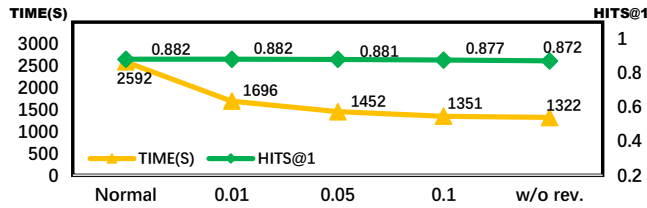


Figure 7: *Hits@1* and time cost of PSR (semi) with different reviewing threshold ϵ on DWY_{DBP-WD} .

Batch Size. To explore the impact of batch size, we report the performances of PSR (semi) with batch size from 128 to 1,024 on DBP_{ZH-EN} and DWY_{DBP-WD} . In this experiment, only the batch size changes, all the other hyper-parameters remain fixed. As shown in Figure 6, our method constantly works well over this wide range of batch sizes on both datasets. Even a small batch size of 128 performs decently, with a drop of less than 2% on *Hits@1*. We observe that the batch size greatly impacts the GPU memory occupation almost linearly. Since PSR adopts a mini-batch training strategy, its space complexity is expected to be only related to batch size and graph density, not to the scale of graphs. The small memory consumption gap between DBP_{15K} and DWY_{100K} indeed verify this expectation.

Embedding Dimension. Figure 6 also reports the performances with embedding dimension d from 100 to 400. Similar to batch size, PSR also works well over this wide range of dimensions. Even a dimension size of 100 performs decently, with a drop of only 3% on *Hits@1*. It is very obvious that both the time and space costs decrease linearly with the shrink of embedding dimension. Overall, PSR is capable of dealing with large-scale datasets and run on devices with limited memory but still output comparable performance.

Incremental Learning. In Section 5.2, we mention that PSR is born with incremental learning ability and propose a simple reviewing strategy to further alleviate "catastrophic forgetting". To validate the effectiveness of our design, we set the reviewing threshold ϵ from 0.01 to 0.1. Furthermore, there are two baselines: (a) *Normal* represents existing EA methods' semi-supervised strategy, i.e., mixing all the newly generated data and early data into the next iteration. (b) *w/o rev.* means not reviewing any early samples at all (i.e., $\epsilon = \infty$). In this way, each pair will be added to the training set only once.

As shown in Figure 7, the performance gap between these two baselines is only 1%, which proves that PSR is capable of learning incrementally. By further incorporating the complete reviewing mechanism, PSR could significantly reduce the time cost while keeping the performance intact. Such an incremental learning strategy could ensure that the training complexity increases linearly with the dataset scale, making massive-scale EA feasible.

Pre-aligned Ratio. In practice, manually annotating pre-aligned entity pairs consumes a lot of resources, especially for large-scale KGs. We expect that the proposed model could keep decent performance with limited pre-aligned entity pairs. To investigate the performance with different pre-aligned ratios, we set the ratios from 10% to 50%. Figure 8 shows the results on DBP_{FR-EN} and

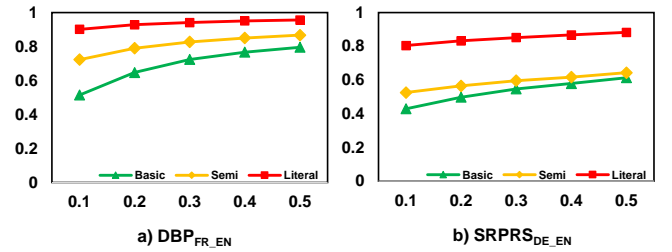


Figure 8: *Hits@1* of PSR with different pre-aligned ratios.

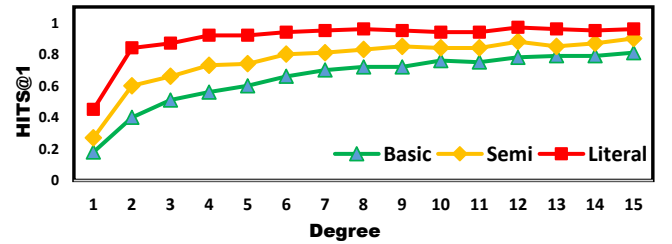


Figure 9: *Hits@1* of the entities with different degrees.

$SRPRS_{DE-EN}$. Benefiting from the rich structure information in DBP_{FR-EN} , the model could iteratively generate a large number of high-quality entity pairs for training. Therefore, the semi-supervised strategy performs pretty well and greatly improves the performance. On the other hand, because $SRPRS_{DE-EN}$ is much more sparse, the impact of the semi-supervised strategy is very limited. In both datasets, introducing literal information could significantly improve the performance. Especially in $SRPRS_{DE-EN}$, literal information could complement the insufficiency of structural information.

Degree Analysis. The above experiments show that the performances of all EA methods on sparse datasets is much worse than that of standard datasets. To further explore the correlation between performance and density, we design an experiment on DBP_{FR-EN} . Figure 9 shows the *Hits@1* of the three variants on different levels of entity degrees. We observe that there is a strong correlation between performance and degree. The semi-supervised strategy does improve the overall performances but has a limited effect on entities whose local structures are extremely sparse. On the other hand, PSR (lit) has much better performances. Unfortunately, literal information is not always available in real-life applications. Therefore, how to better represent these sparse entities without extra information could be one key point for future work.

7 CONCLUSION

In this paper, we prove that the essence of GNNs-based EA methods is to solve a permutation matrix approximately and explain why negative samples are unnecessary from a new angle of view. Furthermore, we propose a novel EA method with three major modifications: (1) Simplified graph encoder with relational graph sampling. (2) Symmetric alignment loss without negative sampling. (3) Incremental semi-supervised learning strategy. Thus, the proposed method could simultaneously possess high performance, high scalability, and high robustness.

REFERENCES

- [1] Antoine Bordes, Nicolas Usunier, Alberto García-Durán, Jason Weston, and Oksana Yakhnenko. 2013. Translating Embeddings for Modeling Multi-relational Data. In *Advances in Neural Information Processing Systems 26: 27th Annual Conference on Neural Information Processing Systems 2013. Proceedings of a meeting held December 5-8, 2013, Lake Tahoe, Nevada, United States*, Christopher J. C. Burges, Léon Bottou, Zoubin Ghahramani, and Kilian Q. Weinberger (Eds.), 2787–2795. <http://papers.nips.cc/paper/5071-translating-embeddings-for-modeling-multi-relational-data>
- [2] Jane Bromley, Isabelle Guyon, Yann LeCun, Eduard Säckinger, and Roopak Shah. 1993. Signature Verification Using a Siamese Time Delay Neural Network. In *Advances in Neural Information Processing Systems 6, [7th NIPS Conference, Denver, Colorado, USA, 1993]*, Jack D. Cowan, Gerald Tesauro, and Joshua Alspector (Eds.), Morgan Kaufmann, 737–744. <http://papers.nips.cc/paper/769-signature-verification-using-a-siamese-time-delay-neural-network>
- [3] Yixin Cao, Zhiyuan Liu, Chengjiang Li, Zhiyuan Liu, Juanzi Li, and Tat-Seng Chua. 2019. Multi-Channel Graph Neural Network for Entity Alignment. In *Proceedings of the 57th Conference of the Association for Computational Linguistics, ACL 2019, Florence, Italy, July 28- August 2, 2019, Volume 1: Long Papers*. 1452–1461. <https://doi.org/10.18653/v1/p19-1140>
- [4] Yixin Cao, Xiang Wang, Xiangnan He, Zikun Hu, and Tat-Seng Chua. 2019. Unifying Knowledge Graph Learning and Recommendation: Towards a Better Understanding of User Preferences. In *The World Wide Web Conference, WWW 2019, San Francisco, CA, USA, May 13-17, 2019*. 151–161. <https://doi.org/10.1145/3308558.3313705>
- [5] Jie Chen, Tengfei Ma, and Cao Xiao. 2018. FastGCN: Fast Learning with Graph Convolutional Networks via Importance Sampling. In *6th International Conference on Learning Representations, ICLR 2018, Vancouver, BC, Canada, April 30 - May 3, 2018, Conference Track Proceedings*. <https://openreview.net/forum?id=rytstxWAW>
- [6] Muhao Chen, Weijia Shi, Ben Zhou, and Dan Roth. 2021. Cross-lingual Entity Alignment with Incidental Supervision. In *Proceedings of the 16th Conference of the European Chapter of the Association for Computational Linguistics: Main Volume, EAACL 2021, Online, April 19 - 23, 2021*, Paola Merlo, Jörg Tiedemann, and Reut Tsarfaty (Eds.), Association for Computational Linguistics, 645–658. <https://www.aclweb.org/anthology/2021.eacl-main.53/>
- [7] Muhao Chen, Yingtao Tian, Mohan Yang, and Carlo Zaniolo. 2017. Multilingual Knowledge Graph Embeddings for Cross-lingual Knowledge Alignment. In *Proceedings of the Twenty-Sixth International Joint Conference on Artificial Intelligence, IJCAI 2017, Melbourne, Australia, August 19-25, 2017*. 1511–1517. <https://doi.org/10.24963/ijcai.2017/209>
- [8] Ting Chen, Simon Kornblith, Mohammad Norouzi, and Geoffrey E. Hinton. 2020. A Simple Framework for Contrastive Learning of Visual Representations. In *Proceedings of the 37th International Conference on Machine Learning, ICML 2020, 13-18 July 2020, Virtual Event (Proceedings of Machine Learning Research, Vol. 119)*. PMLR, 1597–1607. <http://proceedings.mlr.press/v119/chen20j.html>
- [9] Xinlei Chen and Kaiming He. 2020. Exploring Simple Siamese Representation Learning. *CoRR abs/2011.10566* (2020). [arXiv:2011.10566](https://arxiv.org/abs/2011.10566) <https://arxiv.org/abs/2011.10566>
- [10] Wei-Lin Chiang, Xuanqing Liu, Si Si, Yang Li, Samy Bengio, and Cho-Jui Hsieh. 2019. Cluster-GCN: An Efficient Algorithm for Training Deep and Large Graph Convolutional Networks. In *Proceedings of the 25th ACM SIGKDD International Conference on Knowledge Discovery & Data Mining, KDD 2019, Anchorage, AK, USA, August 4-8, 2019*. 257–266. <https://doi.org/10.1145/3292500.3330925>
- [11] Djork-Arné Clevert, Thomas Unterthiner, and Sepp Hochreiter. 2016. Fast and Accurate Deep Network Learning by Exponential Linear Units (ELUs). In *4th International Conference on Learning Representations, ICLR 2016, San Juan, Puerto Rico, May 2-4, 2016, Conference Track Proceedings*. <http://arxiv.org/abs/1511.07289>
- [12] Yanbo Fan, Siwei Lyu, Yiming Ying, and Bao-Gang Hu. 2017. Learning with Average Top-k Loss. In *Advances in Neural Information Processing Systems 30: Annual Conference on Neural Information Processing Systems 2017, December 4-9, 2017, Long Beach, CA, USA*. 497–505. <http://papers.nips.cc/paper/6653-learning-with-average-top-k-loss>
- [13] Matthias Fey, Jan Eric Lenssen, Christopher Morris, Jonathan Masci, and Nils M. Kriege. 2020. Deep Graph Matching Consensus. In *8th International Conference on Learning Representations, ICLR 2020, Addis Ababa, Ethiopia, April 26-30, 2020*. <https://openreview.net/forum?id=HyeJf1HKvS>
- [14] Jean-Bastien Grill, Florian Strub, Florent Althé, Corentin Tallec, Pierre H. Richemond, Elena Buchatskaya, Carl Doersch, Bernardo Ávila Pires, Zhaohan Guo, Mohammad Gheshlaghi Azar, Bilal Piot, Koray Kavukcuoglu, Rémi Munos, and Michal Valko. 2020. Bootstrap Your Own Latent - A New Approach to Self-Supervised Learning. In *Advances in Neural Information Processing Systems 33: Annual Conference on Neural Information Processing Systems 2020, NeurIPS 2020, December 6-12, 2020, virtual*, Hugo Larochelle, Marc'Aurelio Ranzato, Raia Hadsell, Maria-Florina Balcan, and Hsuan-Tien Lin (Eds.). <https://proceedings.neurips.cc/paper/2020/hash/f3ada80d5c4ee70142b17b8192b2958e-Abstract.html>
- [15] Lingbing Guo, Zequn Sun, and Wei Hu. 2019. Learning to Exploit Long-term Relational Dependencies in Knowledge Graphs. In *Proceedings of the 36th International Conference on Machine Learning, ICML 2019, 9-15 June 2019, Long Beach, California, USA*. 2505–2514. <http://proceedings.mlr.press/v97/guo19c.html>
- [16] Raia Hadsell, Sumit Chopra, and Yann LeCun. 2006. Dimensionality Reduction by Learning an Invariant Mapping. In *2006 IEEE Computer Society Conference on Computer Vision and Pattern Recognition (CVPR 2006), 17-22 June 2006, New York, NY, USA*. 1735–1742. <https://doi.org/10.1109/CVPR.2006.100>
- [17] William L. Hamilton, Zitao Ying, and Jure Leskovec. 2017. Inductive Representation Learning on Large Graphs. In *Advances in Neural Information Processing Systems 30: Annual Conference on Neural Information Processing Systems 2017, December 4-9, 2017, Long Beach, CA, USA*, Isabelle Guyon, Ulrike von Luxburg, Samy Bengio, Hanna M. Wallach, Rob Fergus, S. V. N. Vishwanathan, and Roman Garnett (Eds.), 1024–1034. <http://papers.nips.cc/paper/6703-inductive-representation-learning-on-large-graphs>
- [18] Kaiming He, Haoqi Fan, Yuxin Wu, Saining Xie, and Ross B. Girshick. 2020. Momentum Contrast for Unsupervised Visual Representation Learning. In *2020 IEEE/CVF Conference on Computer Vision and Pattern Recognition, CVPR 2020, Seattle, WA, USA, June 13-19, 2020*. IEEE, 9726–9735. <https://doi.org/10.1109/CVPR42600.2020.00975>
- [19] Kaiming He, Xiangyu Zhang, Shaoqing Ren, and Jian Sun. 2016. Deep Residual Learning for Image Recognition. In *2016 IEEE Conference on Computer Vision and Pattern Recognition, CVPR 2016, Las Vegas, NV, USA, June 27-30, 2016*. 770–778. <https://doi.org/10.1109/CVPR.2016.90>
- [20] Thomas N. Kipf and Max Welling. 2016. Semi-Supervised Classification with Graph Convolutional Networks. *CoRR abs/1609.02907* (2016). [arXiv:1609.02907](https://arxiv.org/abs/1609.02907) <https://arxiv.org/abs/1609.02907>
- [21] Guillaume Lample, Alexis Conneau, Marc'Aurelio Ranzato, Ludovic Denoyer, and Hervé Jégou. 2018. Word translation without parallel data. In *6th International Conference on Learning Representations, ICLR 2018, Vancouver, BC, Canada, April 30 - May 3, 2018, Conference Track Proceedings*. OpenReview.net. <https://openreview.net/forum?id=H196sainb>
- [22] Chengjiang Li, Yixin Cao, Lei Hou, Jiaxin Shi, Juanzi Li, and Tat-Seng Chua. 2019. Semi-supervised Entity Alignment via Joint Knowledge Embedding Model and Cross-graph Model. In *Proceedings of the 2019 Conference on Empirical Methods in Natural Language Processing and the 9th International Joint Conference on Natural Language Processing, EMNLP-IJCNLP 2019, Hong Kong, China, November 3-7, 2019*. 2723–2732. <https://doi.org/10.18653/v1/D19-1274>
- [23] Yujia Li, Chenjie Gu, Thomas Dullien, Oriol Vinyals, and Pushmeet Kohli. 2019. Graph Matching Networks for Learning the Similarity of Graph Structured Objects. In *Proceedings of the 36th International Conference on Machine Learning, ICML 2019, 9-15 June 2019, Long Beach, California, USA*. 3835–3845. <http://proceedings.mlr.press/v97/li19d.html>
- [24] Tsung-Yi Lin, Priya Goyal, Ross B. Girshick, Kaiming He, and Piotr Dollár. 2017. Focal Loss for Dense Object Detection. In *IEEE International Conference on Computer Vision, ICCV 2017, Venice, Italy, October 22-29, 2017*. 2999–3007. <https://doi.org/10.1109/ICCV.2017.324>
- [25] Yankai Lin, Zhiyuan Liu, Maosong Sun, Yang Liu, and Xuan Zhu. 2015. Learning Entity and Relation Embeddings for Knowledge Graph Completion. In *Proceedings of the Twenty-Ninth AAAI Conference on Artificial Intelligence, January 25-30, 2015, Austin, Texas, USA*. 2181–2187. <http://www.aaai.org/ocs/index.php/AAAI/AAAI15/paper/view/9571>
- [26] Xin Mao, Wenting Wang, Huimin Xu, Man Lan, and Yuanbin Wu. 2020. MRAEA: An Efficient and Robust Entity Alignment Approach for Cross-lingual Knowledge Graph. In *WSDM '20: The Thirteenth ACM International Conference on Web Search and Data Mining, Houston, TX, USA, February 3-7, 2020*. 420–428. <https://doi.org/10.1145/3336191.3371804>
- [27] Xin Mao, Wenting Wang, Huimin Xu, Yuanbin Wu, and Man Lan. 2020. Relational Reflection Entity Alignment. In *CIKM '20: The 29th ACM International Conference on Information and Knowledge Management, Virtual Event, Ireland, October 19-23, 2020*, Mathieu d'Aquin, Stefan Dietze, Claudia Hauff, Edward Curry, and Philippe Cudré-Mauroux (Eds.), ACM, 1095–1104. <https://doi.org/10.1145/3340531.3412001>
- [28] Yunqi Qiu, Yuanzhuo Wang, Xiaolong Jin, and Kun Zhang. 2020. Stepwise Reasoning for Multi-Relation Question Answering over Knowledge Graph with Weak Supervision. In *WSDM '20: The Thirteenth ACM International Conference on Web Search and Data Mining, Houston, TX, USA, February 3-7, 2020*. 474–482. <https://doi.org/10.1145/3336191.3371812>
- [29] Michael Sejr Schlichtkrull, Thomas N. Kipf, Peter Bloem, Rianne van den Berg, Ivan Titov, and Max Welling. 2018. Modeling Relational Data with Graph Convolutional Networks. In *The Semantic Web - 15th International Conference, ESWC 2018, Heraklion, Crete, Greece, June 3-7, 2018, Proceedings*. 593–607. https://doi.org/10.1007/978-3-319-93417-4_38
- [30] Florian Schroff, Dmitry Kalenichenko, and James Philbin. 2015. FaceNet: A unified embedding for face recognition and clustering. In *IEEE Conference on Computer Vision and Pattern Recognition, CVPR 2015, Boston, MA, USA, June 7-12, 2015*. IEEE Computer Society, 815–823. <https://doi.org/10.1109/CVPR.2015.7298682>

- [31] Zequn Sun, Muhao Chen, Wei Hu, Chengming Wang, Jian Dai, and Wei Zhang. 2020. Knowledge Association with Hyperbolic Knowledge Graph Embeddings. In *Proceedings of the 2020 Conference on Empirical Methods in Natural Language Processing, EMNLP 2020, Online, November 16–20, 2020*, Bonnie Webber, Trevor Cohn, Yulan He, and Yang Liu (Eds.). Association for Computational Linguistics, 5704–5716. <https://doi.org/10.18653/v1/2020.emnlp-main.460>
- [32] Zequn Sun, Wei Hu, and Chengkai Li. 2017. Cross-Lingual Entity Alignment via Joint Attribute-Preserving Embedding. In *The Semantic Web - ISWC 2017 - 16th International Semantic Web Conference, Vienna, Austria, October 21–25, 2017, Proceedings, Part I (Lecture Notes in Computer Science, Vol. 10587)*, Claudia d'Amato, Miriam Fernández, Valentina A. M. Tamma, Freddy Lécué, Philippe Cudré-Mauroux, Juan F. Sequeda, Christoph Lange, and Jeff Heflin (Eds.). Springer, 628–644. https://doi.org/10.1007/978-3-319-68288-4_37
- [33] Zequn Sun, Wei Hu, Qingheng Zhang, and Yuzhong Qu. 2018. Bootstrapping Entity Alignment with Knowledge Graph Embedding. In *Proceedings of the Twenty-Seventh International Joint Conference on Artificial Intelligence, IJCAI 2018, July 13–19, 2018, Stockholm, Sweden*. 4396–4402. <https://doi.org/10.24963/ijcai.2018/611>
- [34] Zequn Sun, JiaCheng Huang, Wei Hu, Muchao Chen, Lingbing Guo, and Yuzhong Qu. 2020. TransEdge: Translating Relation-contextualized Embeddings for Knowledge Graphs. *CoRR* abs/2004.13579 (2020). arXiv:2004.13579 <https://arxiv.org/abs/2004.13579>
- [35] Zequn Sun, Chengming Wang, Wei Hu, Muhao Chen, Jian Dai, Wei Zhang, and Yuzhong Qu. 2020. Knowledge Graph Alignment Network with Gated Multi-Hop Neighborhood Aggregation. In *The Thirty-Fourth AAAI Conference on Artificial Intelligence, AAAI 2020, The Thirty-Second Innovative Applications of Artificial Intelligence Conference, IAAI 2020, The Tenth AAAI Symposium on Educational Advances in Artificial Intelligence, EAAI 2020, New York, NY, USA, February 7–12, 2020*. 222–229. <https://aaai.org/ojs/index.php/AAAI/article/view/5354>
- [36] Petar Velickovic, Guillem Cucurull, Arantxa Casanova, Adriana Romero, Pietro Liò, and Yoshua Bengio. 2018. Graph Attention Networks. In *6th International Conference on Learning Representations, ICLR 2018, Vancouver, BC, Canada, April 30 - May 3, 2018, Conference Track Proceedings*. <https://openreview.net/forum?id=rJXMpikCZ>
- [37] Hongwei Wang, Fuzheng Zhang, Miao Zhao, Wenjie Li, Xing Xie, and Minyi Guo. 2019. Multi-Task Feature Learning for Knowledge Graph Enhanced Recommendation. In *The World Wide Web Conference, WWW 2019, San Francisco, CA, USA, May 13–17, 2019*. 2000–2010. <https://doi.org/10.1145/3308558.3313411>
- [38] Zhichun Wang, Qingsong Lv, Xiaohan Lan, and Yu Zhang. 2018. Cross-lingual Knowledge Graph Alignment via Graph Convolutional Networks. In *Proceedings of the 2018 Conference on Empirical Methods in Natural Language Processing, Brussels, Belgium, October 31 - November 4, 2018*. 349–357. <https://doi.org/10.18653/v1/d18-1032>
- [39] Yuting Wu, Xiao Liu, Yansong Feng, Zheng Wang, Rui Yan, and Dongyan Zhao. 2019. Relation-Aware Entity Alignment for Heterogeneous Knowledge Graphs. In *Proceedings of the Twenty-Eighth International Joint Conference on Artificial Intelligence, IJCAI 2019, Macao, China, August 10–16, 2019*. 5278–5284. <https://doi.org/10.24963/ijcai.2019/733>
- [40] Yuting Wu, Xiao Liu, Yansong Feng, Zheng Wang, and Dongyan Zhao. 2019. Jointly Learning Entity and Relation Representations for Entity Alignment. In *Proceedings of the 2019 Conference on Empirical Methods in Natural Language Processing and the 9th International Joint Conference on Natural Language Processing, EMNLP-IJCNLP 2019, Hong Kong, China, November 3–7, 2019*. 240–249. <https://doi.org/10.18653/v1/D19-1023>
- [41] Kun Xu, Liwei Wang, Mo Yu, Yansong Feng, Yan Song, Zhiguo Wang, and Dong Yu. 2019. Cross-lingual Knowledge Graph Alignment via Graph Matching Neural Network. In *Proceedings of the 57th Conference of the Association for Computational Linguistics, ACL 2019, Florence, Italy, July 28- August 2, 2019, Volume 1: Long Papers*. 3156–3161. <https://doi.org/10.18653/v1/p19-1304>
- [42] Hsiu-Wei Yang, Yanyan Zou, Peng Shi, Wei Lu, Jimmy Lin, and Xu Sun. 2019. Aligning Cross-Lingual Entities with Multi-Aspect Information. In *Proceedings of the 2019 Conference on Empirical Methods in Natural Language Processing and the 9th International Joint Conference on Natural Language Processing, EMNLP-IJCNLP 2019, Hong Kong, China, November 3–7, 2019*. 4430–4440. <https://doi.org/10.18653/v1/D19-1451>
- [43] Hanqing Zeng, Hongkuan Zhou, Ajitesh Srivastava, Rajgopal Kannan, and Viktor K. Prasanna. 2020. GraphSAINT: Graph Sampling Based Inductive Learning Method. In *8th International Conference on Learning Representations, ICLR 2020, Addis Ababa, Ethiopia, April 26–30, 2020*. <https://openreview.net/forum?id=BJe8pkHFwS>
- [44] Chen Zhao, Chenyan Xiong, Xin Qian, and Jordan L. Boyd-Graber. 2020. Complex Factoid Question Answering with a Free-Text Knowledge Graph. In *WWW '20: The Web Conference 2020, Taipei, Taiwan, April 20–24, 2020*. 1205–1216. <https://doi.org/10.1145/3366423.3380197>
- [45] X. Zhao, W. Zeng, J. Tang, W. Wang, and F. Suchanek. 2020. An Experimental Study of State-of-the-Art Entity Alignment Approaches. *IEEE Transactions on Knowledge and Data Engineering* (2020), 1–1.
- [46] Qiannan Zhu, Xiaofei Zhou, Jia Wu, Jianlong Tan, and Li Guo. 2019. Neighborhood-Aware Attentional Representation for Multilingual Knowledge Graphs. In *Proceedings of the Twenty-Eighth International Joint Conference on Artificial Intelligence, IJCAI 2019, Macao, China, August 10–16, 2019*. 1943–1949. <https://doi.org/10.24963/ijcai.2019/269>